https://doi.org/10.5194/egusphere-2026-1385
Preprint. Discussion started: 19 March 2026

The climate-ice sheet interactions at the Late Ordovician glaciation onset revealed by numerical simulations

Yudong Sun[1], Yonggang Liu[1], Jiacheng Wu[1], Kai Man[1], Haonan Yu[1], Shuai Yuan[1], Qi Cui[1], Yue Liu[1], Yizhang Liu[1], Qiang Wei[2], Yongyun Hu[1]

[1]Department of Atmospheric and Oceanic Sciences, School of Physics, Peking University, Beijing, 100871, China
[2]State Key Laboratory of Tibetan Plateau Earth System, Resources & Environment, Institute of Tibetan Plateau Research, Chinese Academy of Sciences, Beijing, 100101, China

Correspondence to: Yongyun Hu (yyhu@pku.edu.cn), Qiang Wei (qwei@itpcas.ac.cn)

Abstract. The Late Ordovician marks the first major continental ice sheet event in the Phanerozoic Eon, coinciding with a dramatic global temperature drop and one of the largest mass extinctions. However, the critical role of ice sheet-climate feedbacks in driving the Late Ordovician glaciation remains poorly understood. Using an asynchronous coupling approach, we systematically analyze the feedback processes between the ice sheets and the climate system. The coupled simulations reveal a key positive feedback loop: ice sheet growth triggers katabatic winds, which in turn promote further ice sheet expansion. Results show a 1.5 °C decrease in global mean surface temperature caused by ice sheet onset, with significant cooling over mid- to high-latitude continents while warming over global oceans. The ocean warming is driven by the atmospheric stationary wave triggered by the massive ice sheet on the Gondwana continent. Our findings provide new insights into the mechanisms underlying the "Early Palaeozoic Ice Age" paradigm and highlight the complex interactions between ice sheet dynamics, atmospheric and ocean circulation, emphasizing the importance of incorporating coupled ice sheet-climate feedbacks in palaeoclimate simulations.

1 Introduction

The Late Ordovician (approximately 458-440 million years ago; Ma), marked by the first continental ice sheet growth event in the Phanerozoic Eon (Finnegan et al., 2011; Trotter et al., 2008), has long attracted the interest of palaeogeographers and palaeoclimatologists. This period is considered one of the most unique, contradictory, and enigmatic, with dramatic environmental changes. Studies have shown that atmospheric CO_2 levels (pCO_2) during this time may have been 8 to 20 times higher than the preindustrial (PI) atmospheric level (PAL, 1 PAL=280 ppmv) (Berner, 1994), while coinciding with a significant glaciation event and a severe cooling of the climate that probably had a profound impact on global biodiversity (Bergmann et al., 2025; Caputo and Crowell, 1985; Cocks and Torsvik, 2021; Holmden et al., 2013; Saupe et al., 2020; Trotter et al., 2008). During the Late Ordovician, particularly the Hirnantian (~445-443 Ma), strong evidence indicates that the ice sheet had extended as far as 40° S (Cocks and Torsvik, 2021; Finnegan et al., 2011; Pohl et al., 2016; Torsvik and Cocks, 2016). Concurrently, reconstructions suggest a temperature drop of more than 8 °C in tropical sea surface

https://doi.org/10.5194/egusphere-2026-1385
Preprint. Discussion started: 19 March 2026

temperatures (SSTs) from the Middle Ordovician, reaching temperature conditions of present-day levels, thereby entering an icehouse state (Melchin et al., 2013; Trotter et al., 2008). Additionally, the Late Ordovician witnessed one of the largest mass extinctions in the Phanerozoic, with nearly 85 % of marine species dying out (Saupe et al., 2020; Sheehan, 2001; Trotter et al., 2008).

During this time, the continents were mostly concentrated in the Southern Hemisphere (SH), connected to form the Gondwana supercontinent. Earlier studies have explored, through reconstructions and simulations, the influence of pCO_2 or other boundary factors on the development of the super ice sheet (Crowley et al., 1987; Crowley and Baum, 1991, 1995; Delabroye and Vecoli, 2010; Finnegan et al., 2011; Herrmann et al., 2004; Holmden et al., 2013; Horton et al., 2007; Pohl et al., 2016, 2021; Saupe et al., 2020; Vandenbroucke et al., 2009). Most studies suggest that the pCO_2 required to trigger glaciation might be far higher than PI levels (Berner, 1994; Herrmann et al., 2004; Li et al., 2022; Pohl et al., 2016). Additionally, the extent of the ice sheet coverage was not highly sensitive to continental topography, elevation, and basal friction (Pohl et al., 2016).

A challenging issue is the lack of discussions on the mechanisms behind ice sheet growth, despite many studies analysing physical evidence and simulation results. This gap has limited our understanding of key processes during largescale glaciations (Pollard, 2010). A major obstacle to understanding ice sheet growth mechanisms is the inadequate coupling of ice sheet models and climate models, which fail to capture the critical feedbacks between the cryosphere and climate, occurring through a variety of interconnected processes and feedbacks (Fyke et al., 2018; Pollard, 2010).

Some insights on the climate-ice sheet interaction have actually been indirectly derived from the offline ice sheet simulations (Fyke et al., 2018; Gregoire et al., 2016; Hakuba et al., 2012; Löfverström and Liakka, 2016; Oerlemans, 1981; Scherrenberg et al., 2023). When an external perturbation increases ice volume, the ice margin tends to advance downslope, expanding the ice surface into zones prone to ablation. The resulting increase in melt can offset the initial mass gain, allowing the ice sheet to approach a new equilibrium. If, however, the background climate provides insufficient horizontal temperature gradients to amplify ablation and halt margin advance, the ice sheet may continue to expand into warmer and/or drier climate regimes, or advance to the coastline, until further growth is no longer sustainable (Fyke et al., 2018; Oerlemans, 1981). Other processes then layer onto this core mechanism, making the response highly nonlinear, strongly region-dependent, and tightly coupled across the other components of the earth system (Hakuba et al., 2012; Löfverström and Liakka, 2016; Pohl et al., 2016; Scherrenberg et al., 2023).

Changes in topography due to ice growth can reshape the spatial patterns of temperature and precipitation (Fyke et al., 2018), which in turn may affect the surface mass balance (SMB) of ice sheet and thus ice growth. This effect has been shown to play an important role in the evolution of the Laurentide Ice Sheet (LIS) in the Last Glacial Maximum (LGM) (Gong et al., 2015; Gregoire et al., 2018; Klockmann et al., 2020; Löfverström and Liakka, 2016; Pausata et al., 2011; Zhu et al., 2014); A higher elevation of LIS strengthens the wind-driven gyre circulation in the North Atlantic, leading to a poleward shift of the sea ice edge and warmer the subpolar North Atlantic region which may prevents further growth of LIS. Moreover, several studies have demonstrated that the LIS can significantly alter the atmospheric stationary wave fields, which in turn

https://doi.org/10.5194/egusphere-2026-1385
Preprint. Discussion started: 19 March 2026

influences local temperature and precipitation anomalies critical to the surface mass balance (Lee et al., 2023; Liakka et al., 2016; Liakka and Lofverstrom, 2018).

Although some of the climate-ice sheet interactions can be reasonably and qualitatively inferred from offline modelling, they cannot be captured in a consistent way and some interactions may be missed. Coupled modelling is essential for a complete and quantitative understanding of the climate-ice sheet interactions (Horton et al., 2010; Pohl et al., 2016; Wei et al., 2023). Horton et al. (2010), basing on transient simulations, emphasized the critical role of vegetation-ice sheet coupling in reproducing the orbitally driven sea level fluctuations in the geological records of the late Palaeozoic. They found that ice sheet advances coincided with high-latitude tundra expansion during low insolation, while retreats were linked to the spread of barren land near the ice margin under high insolation. Wei et al. (2023) showed that the growth of glaciers along the western and southern boundaries of the Tibetan Plateau during the LGM intercepted horizontal moisture transport, and reduced the glacier coverage and increased the surface temperature of the plateau interior. Pohl et al. (2016) demonstrated that coupled models effectively amplify the nonlinear relationship between the Late Ordovician ice sheets and pCO_2, allowing for the development of extensive land-based ice sheets under high pCO_2 conditions. However, they did not systematically go into analysing the mechanisms behind the ice sheet expansion, a gap that this study fills by providing key insights.

Here we use an asynchronous coupling approach to link an ice sheet model with a fully coupled atmosphere-ocean general circulation model. In doing so, we are able to systematically analyze the feedback processes between the ice sheets and climate, as well as their profound and unexpected impacts on ocean circulation and SSTs, achieving a high level of agreement with geological records. The structure of this paper is as follows. Sect. 2 outlines the models and asynchronous coupling methods. In Sect. 3, we compare the ice sheet extent of the offline simulation with the coupled simulation, analysing the limiting factors for ice sheet growth from the perspectives of accumulation and ablation. We then discuss the ice sheet-climate feedbacks and their impact on the climate system, and the simulation evidence for the "Early Palaeozoic Ice Age" paradigm (Pohl et al., 2016). Finally, in Sect. 4, we provide a conclusion and outlook for future research.

2 Methods: models and configuration

2.1 Climate model

The deep-time climate simulations in this study were performed using the Community Earth System Model version 1.2.2 (CESM 1.2.2), developed by the National Center for Atmospheric Research (NCAR) (Hurrell et al., 2013). CESM 1.2.2 is a fully coupled global Earth system model that integrates the atmosphere (Community Atmosphere Model version 4, CAM4), land (Community Land Model version 4, CLM4), ocean (Parallel Ocean Program version 2, POP2), sea ice (Community Ice CodE version 4, CICE4), and ice sheet (Community Ice Sheet Model, CISM) components through a central coupler. Although the model includes an ice sheet component, its functionality is currently limited and does not officially support two-way coupling, meaning that glacier and ice sheet evolution cannot feed back to the rest of the climate system. Therefore,

https://doi.org/10.5194/egusphere-2026-1385
Preprint. Discussion started: 19 March 2026

the ice sheet module in CESM, CISM, was deactivated in the present simulations. The land component, CLM4, incorporates the carbon–nitrogen model with dynamic vegetation (CNDV) (Thornton et al., 2007) to simulate the spatial distribution and physiological responses of vegetation.

The model configurations are summarized as follows. The atmospheric component uses a horizontal resolution of 3.75°×3.75° (T31) with 26 vertical levels. The ocean component is configured on the g37 grid, which features a uniform longitudinal spacing (3°) and a variable latitudinal spacing (~0.6° at the equator and ~0.9° at high latitudes) with 60 vertical levels. The sea-ice model shares the same horizontal grid as the ocean, while the land model shares the same horizontal grid as the atmosphere. pCO_2 is prescribed at 6 PAL so that the simulated global mean surface temperature (GMST) by CESM1.2.2 matches the reconstructed one for the Late Ordovician (Li et al., 2022; Scotese et al., 2021). Earth's orbital parameters are set to the PI values. Land-sea distribution and topography are derived from the reconstruction of Scotese and Wright (2018) for 440 Ma (Fig. 1). The solar constant is set to 1313 W m^{-2}, approximately 3.5 % weaker than that of the present day (Li et al., 2022; Warthen, 2016). These settings follow the Phanerozoic palaeoclimate simulations of Li et al. (2022), whose 440 Ma experiment is adopted as the control simulation in this study to ensure consistent boundary conditions for ice sheet–climate coupling experiments.

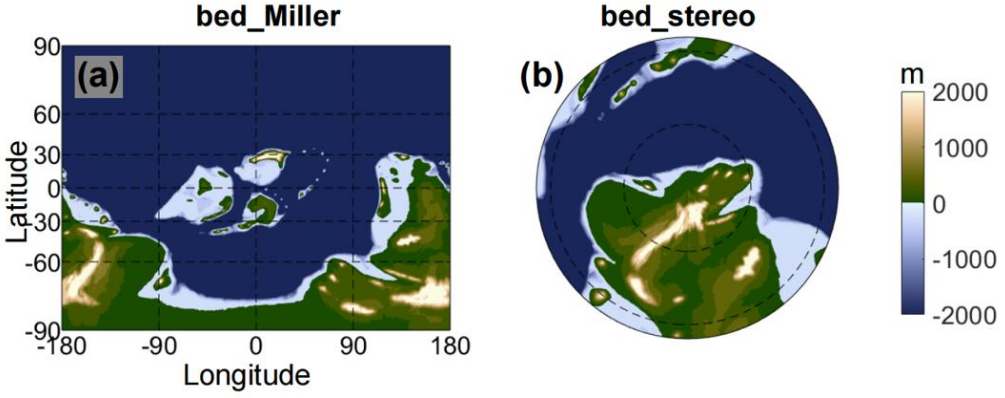

Figure 1: Late Ordovician palaeogeography. (a) Late Ordovician palaeogeography under the Miller projection. **(b)** As (a), but with a stereographic projection centered at the South Pole.

2.2 Ice sheet model

The simulations of continental ice sheets were performed using the Ice-sheet and Sea-level System Model version 4.23 (ISSM 4.23), jointly developed by NASA Jet Propulsion Laboratory (JPL) and the University of California, Irvine (UCI) (Larour et al., 2012). ISSM is a finite-element, thermo-mechanically coupled ice sheet model that solves the mass, momentum, and energy balance equations on an unstructured mesh. In this study, the model is configured at a horizontal resolution of 60 km with 15 vertical levels, and the dynamical core is based on the Shallow Ice Approximation (SIA). The

https://doi.org/10.5194/egusphere-2026-1385
Preprint. Discussion started: 19 March 2026

basal melt rate beneath floating ice shelves is prescribed at 0.1 m yr^{-1}, within the range commonly adopted in previous Antarctic ice sheet studies (Pollard and DeConto, 2012).

ISSM uses monthly mean surface temperature and precipitation from the CESM simulations to calculate surface mass balance. Surface accumulation is directly derived from the frozen fraction of precipitation, while ablation is calculated using the Positive Degree-Day (PDD) method (see more details from Appendix A), and superimposed ice formation is represented by a parameterization scheme. In all PDD-based calculations, a standard deviation (σ) of 5.5 °C is applied to account for monthly air temperature variability (Reeh, 1991). The PDD approach assumes that near-surface air temperature controls melt processes through an empirical relationship with the melting point. Despite its simplicity, this scheme has been demonstrated to reproduce large-scale ice sheet behaviour effectively and efficiently. For the basal friction formulation, the Paterson-type sliding law is employed, with parameter values calibrated to best reproduce modern Antarctic ice volume and flow patterns (Man et al., 2023).

2.3 Asynchronous coupling between the climate and ice sheet models

An asynchronous coupling strategy (Wei et al., 2023) was employed to link the climate model (CESM) and the ice sheet model (ISSM). In this approach, CESM and ISSM exchange boundary conditions at discrete coupling intervals, allowing each model to evolve independently over its characteristic timescale. During each coupling cycle, surface elevation and surface type in CESM (e.g., transitions among vegetation, bare ground, wetlands, and glaciers) are updated according to the evolving ice sheet geometry and extent. Conversely, ISSM is forced by monthly mean surface temperature and precipitation fields from CESM to perform thermo-mechanical and dynamical simulations of ice sheet growth and retreat. The simulations are initialized from the 440 Ma control experiment of Li et al. (2022), and the ice sheet model evolves from an ice-free initial state to equilibrium conditions. The coupling frequency is designed such that the ratio of climate to ice sheet model time steps is approximately 10:2500, corresponding to one coupling exchange every 10 CESM years, during which ISSM integrates independently for 2500 model years. The total integration time of the ice sheet model is 200 ka (i.e., eighty coupling cycles). Equilibrium is diagnosed based on the stabilization of global mean top-of-atmosphere (TOA) net radiation (< 0.1 W m^{-2}) and GMST (the trend of drifting < 0.2 °C yr^{-1} during the final 100 years) in CESM, together with changes in ice sheet extent and thickness (< 1 % during the last coupling interval) simulated by ISSM. The equilibrium state and selected intermediate snapshots are subsequently analyzed to investigate the coupled climate–ice sheet interactions.

2.4 Experiments

In previous uncoupled ice sheet-climate simulations, the feedback of ice sheets to climate was normally considered by simply adjusting temperature and precipitation forcings by lapse rate and glacial desertification effects, respectively, which then affect ice sheet growth and evolution (Herrmann et al., 2004; Vizcaíno et al., 2010). While this method of forcing can partially reflect the impact of ice sheets on the local climate, it does not fully capture the feedback between the cryosphere's evolution and the other components of the Earth system. For comparison with such traditional method, we first run an offline

https://doi.org/10.5194/egusphere-2026-1385
Preprint. Discussion started: 19 March 2026

ice sheet simulation using the equilibrium results from the climate model under pCO_2 of 6 PAL. Then, a coupled simulation is carried out under the same CO_2 level. In the coupled simulation, the evolution of ice sheet affects surface topography, albedo, and atmospheric and oceanic circulations. These changes, in turn, modify the temperature and precipitation fields that drive ice sheet growth, thereby regulating its stability and expansion.

To further isolate the respective roles of the ocean and atmosphere in mediating the climatic impact of the ice sheet, two additional sets of experiments are carried out. In one of them, global SST is prescribed to that of the control run, while in the other, the ocean is run in a slab ocean mode (SOM). In the SOM experiments, the ocean heat transport is prescribed as in the control experiment of Li et al. (2022). Each set were performed with a large continental ice sheet obtained from the equilibrium state of the fully coupled simulation and fixed throughout. The prescribed-SST simulations allow us to extract the direct influence of ice sheet on atmospheric circulation, while the SOM simulations allow us to distinguish between the contributions of ocean heat transport and surface heat exchange to the temperature anomalies observed in the fully coupled experiment. These two sets of experiments are all run for 300 years, and the last 100 years are used for analyzes.

3 Results and discussion

3.1 the Late Ordovician ice sheet

In the offline simulation where ice sheet-climate feedbacks are not considered, the results align with those of previous studies (Herrmann et al., 2004; Lowry et al., 2014; Pohl et al., 2016): the ice sheet is confined to high-latitude regions (≥ 60° S), showing significant discrepancies with the geological tillite records (Cocks and Torsvik, 2021) (Fig. 2). Because the climate condition is comparable to that of reconstruction, the flawed results of the offline ice sheet simulation should not be primarily due to the overestimated surface temperature, but rather the failure of a one-way forcing framework to capture the cryosphere's feedback on the climate system. The comparison with the coupled simulation, discussed in the following paragraphs, will further support this view. Lowering pCO_2 might reproduce an ice sheet extent in the offline simulations that is consistent with the geological records (Pohl et al., 2016). Tests show that pCO_2 needs to be lowered to ~1 PAL (Fig. B1) with the corresponding GMST lowered to ~6 °C, which is far lower than that of the reconstructions (~15 °C) (Li et al., 2022; Scotese et al., 2021; Trotter et al., 2008). Therefore, this approach contradicts the geological constraints on both pCO_2 levels and GMST for the Late Ordovician, in which a super ice sheet formed under a relatively warm climate.

https://doi.org/10.5194/egusphere-2026-1385
Preprint. Discussion started: 19 March 2026

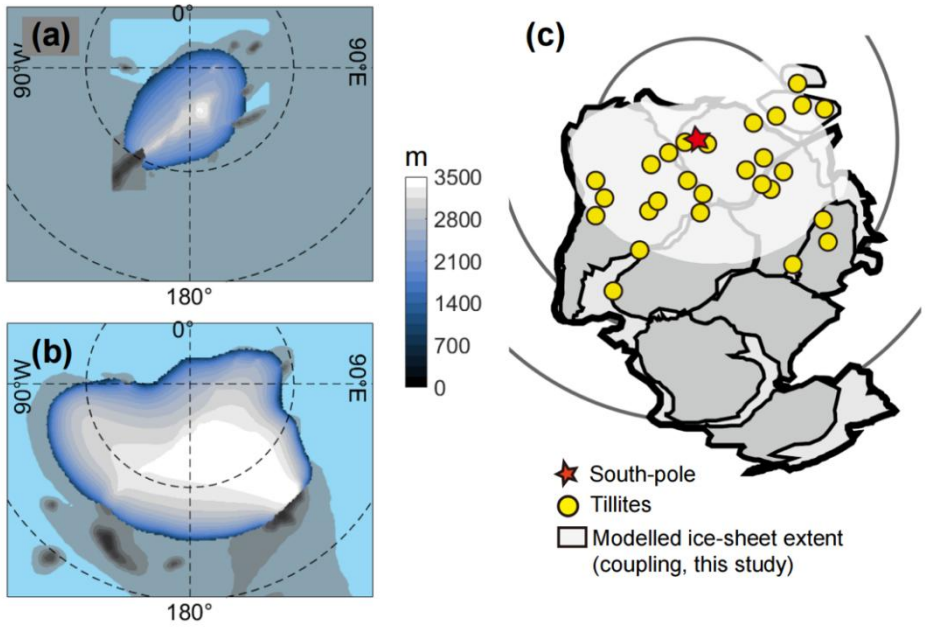

Figure 2: Late Ordovician glacial tillites, and ice sheet surface. (a) Equilibrium result of the ice sheet surface topography (blue-grey color) simulated by the offline method at 6 PAL. The bedrock topography is indicated by grey scale whose colorbar is not shown here but more details can be found in Fig. 1. **(b)** As (a), but with coupled climate and ice sheet models. Latitude is shown at 30° intervals. **(c)** Locations of glacial deposits.

Figure 2b shows the surface topography of the ice sheet in the coupled simulation at equilibrium. Compared to the uncoupled scenario, the ice sheet not only forms along the Antarctic mountain range but also extends significantly toward lower latitudes (~40° S), nearly covering the entire southern portion of Gondwana. This result closely matches the distribution of glacial tillites in the geological record (Cocks and Torsvik, 2021; Pohl et al., 2016) (Fig. 2c), demonstrating a high degree of spatial consistency. This result suggests that considering ice-climate feedback is crucial for realistically reproducing the formation and distribution of large-scale ice sheets during the relatively warm Late Ordovician.

While many studies suggest that grounded ice sheets likely connected into a whole massive ice sheet during the peak of the Hirnantian glaciation (the "large scenario"), the hypothesis of disconnected ice sheets (the "small scenario") has still garnered support in some research (Finnegan et al., 2011). Consistent with much of the modelling work, our results support the idea that a single, large ice sheet covered the entire mid- to high-latitude supercontinent during the Late Ordovician glaciation. The total volume of the ice sheet obtained here corresponds to a sea level drop of ~180 m, close to the levels during the LGM (Montañez and Poulsen, 2013), which is consistent with previous reconstructions. In contrast, the volume of scattered glaciers would be much smaller, and their contribution to sea level changes relatively lower (Horton et al., 2010).

The coupled simulation reveals that the ice sheet-climate system exhibits a characteristic equilibration timescale of approximately 80 ka (Fig. B2). This timescale is much longer than those of the precession (~21,000 years) and obliquity (~41,000 years) cycles, probably implying a relative insensitivity of the Late Ordovician ice sheet to orbital forcing. The

https://doi.org/10.5194/egusphere-2026-1385
Preprint. Discussion started: 19 March 2026

asynchronous coupling method employed both here and Pohl et al. (2016), however, may not accurately capture response timescales of the ice sheet. Future studies using synchronously coupled frameworks or much shorter coupling steps for the ice sheet model will be essential to elucidate the response of Late Ordovician ice sheet to orbital forcing.

Most previous modelling studies of Late Ordovician continental glaciation used the offline method (Crowley et al., 1987; Crowley and Baum, 1991, 1995; Herrmann et al., 2004; Horton et al., 2007; Lowry et al., 2014; Pohl et al., 2016, 2021; Vandenbroucke et al., 2009), with Pohl et al. (2016) being the only one that did coupled simulations. Offline simulations generally needed quite low pCO_2 to produce an ice sheet comparable to the reconstructions. For example, the simulated ice sheet remained largely confined within the polar circle in Lowry et al. (2014) even at pCO_2 as low as 2 PAL. Pohl et al. (2016) did both offline and coupled simulations, using climate and ice-sheet models distinct from those used in this study and with a much lower coupling frequency (200 ka) and coarser model resolution (4.5°×7.5°). In their simulations, a sufficiently large ice sheet could not be obtained in the offline mode until pCO_2 was dropped to 3 PAL while it could be obtained in the coupled mode when pCO_2 was as high as 12 PAL. Our results of the offline experiment at 6 PAL are most comparable in areal coverage to their 10 PAL offline simulation, possibly due to differences in boundary conditions (e.g., topography, land-sea configuration, vegetation cover) and model structure. Thus, our results are broadly consistent with those of Pohl et al. (2016). However, Pohl et al. (2016) did not explicitly analyze the feedback mechanisms through which coupling facilitates ice-sheet growth. Identifying and quantifying these processes is a primary objective of the present study and is addressed in the following sections.

3.2 Limiting factors for ice sheet growth

The process of ice sheet development shown in Fig. 3g-i indicates that during the initial stage of ice sheet expansion, a small, elongated land-based ice sheet first forms, extending roughly from 80° S to 60° S, along the mountain range at the southern end of Gondwana (Fig. 1). The presence of the mountains lowers the surface temperature and facilitates the initial growth of the ice sheet. The ice sheet expands to an extent similar to the equilibrium state of the offline simulation (Fig. 2a) in approximately 10 ka. Subsequently, the ice sheet grows outward from the mountain range, gradually expanding toward the continental margins and the low-latitude interior of the supercontinent, eventually reaching approximately 40° S, almost completely covering the southern portion of Gondwana. The overall shape of the ice sheet is dome-like, centered on the interior of the supercontinent, constrained by continental boundaries in the high latitude and the 40° S line in the mid-latitude continental interior. Notably, in this simulation with pCO_2 = 6 PAL, large ice shelves do not form in any of the time periods, even around the high-latitude polar seas. This coincides with the absence of large-scale sea ice.

https://doi.org/10.5194/egusphere-2026-1385
Preprint. Discussion started: 19 March 2026

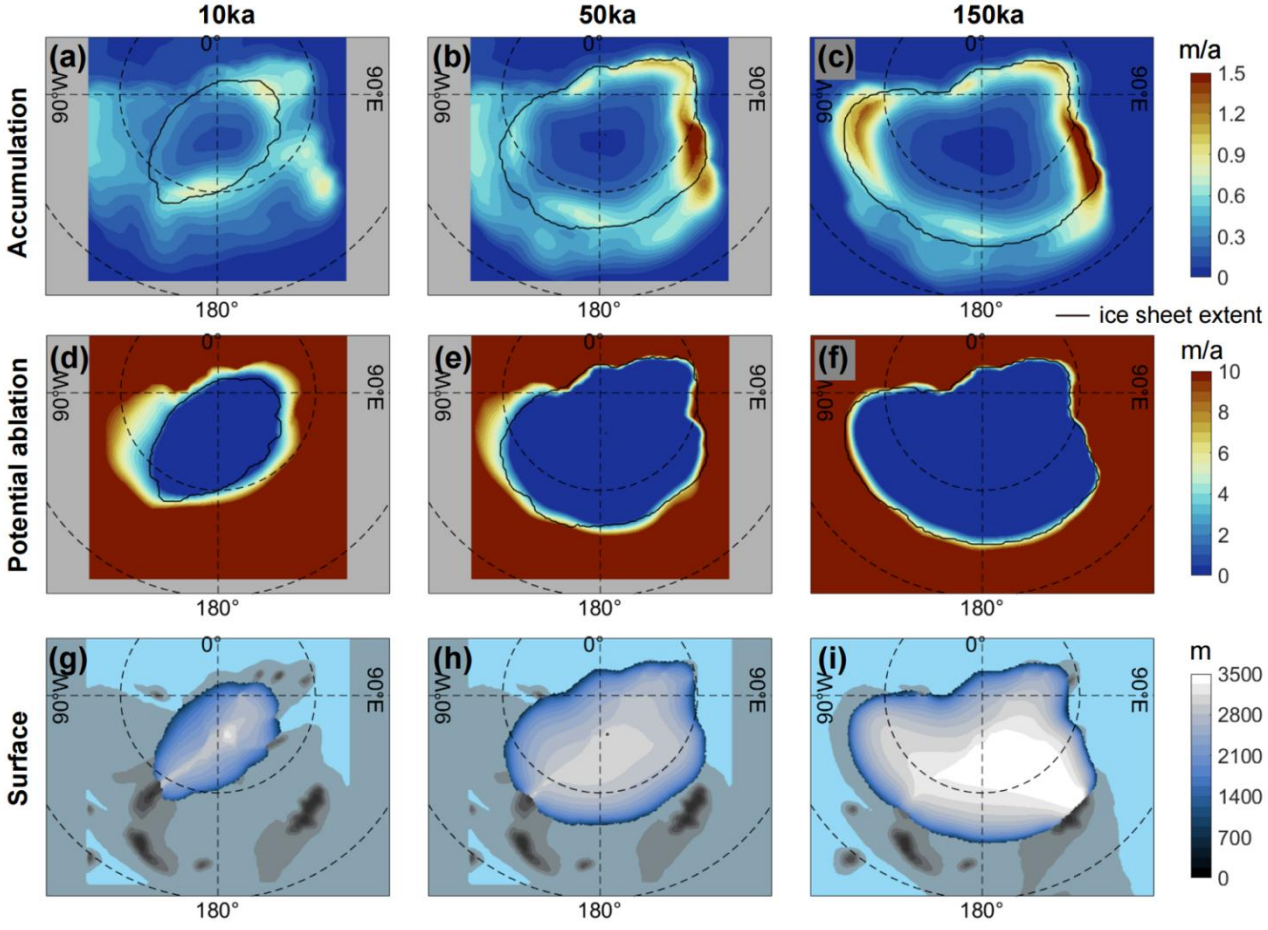

Figure 3: Contribution of accumulation and ablation to ice sheet growth. Three snapshots from the coupled framework simulation at **(a, d, g)** 10 ka, **(b, e, h)** 50 ka, and **(c, f, i)** 150 ka. Latitude is shown at 30° intervals.

Inspection of glacier dynamics suggests that precipitation was not the limiting factor for the growth of land-based ice sheets during the Late Ordovician glaciation (Fig. 3a-c), unlike that for the Tibetan Plateau during the LGM (Wei et al., 2023). In fact, during the development of the ice sheet, precipitation was almost never lacking over the growth zone near the ice sheet front (Fig. B3). This is probably because the mid-latitude moisture transport was powerful under a relatively warm climate state while the mountain range was neither high nor extensive enough for its blocking effect to substantially cut off the moisture supply. For the Late Ordovician, it is the high temperature that is preventing the ice sheet from expanding in the offline simulation (Fig. 3a). In our coupled simulation, the growth of an ice sheet lowers the surface temperature of the surrounding region, expanding the region of low ablation (compare the low-ablation zone to the ice edge (black curve) in Fig. 3d-f). As the ice sheet expands, the low-ablation region also extends outwards, until the ice sheet reaches low enough latitudes (~40° S), where the temperature is too high so that the ablation remains high even right at the edge of ice sheet (Fig. 3f).

https://doi.org/10.5194/egusphere-2026-1385
Preprint. Discussion started: 19 March 2026

3.3 The katabatic winds

The surface cooling in the coupled simulation is realized by katabatic winds which blow downslope along the ice sheet's surface. The katabatic wind is a gravity-driven cold air advection phenomenon that is commonly observed in polar and mountainous regions (Parish and Cassano, 2003; Vihma et al., 2011), like Antarctica, the Greenland ice sheet, and the Alps. Taking Antarctica as an example, the long polar night causes the surface to cool continuously, dramatically lowering near-surface air temperatures and creating a stable cold air layer (Connolley, 1996). Due to the high elevation and steep slopes near its edges, cold air accelerates downslope under gravity, with wind speeds sometimes exceeding 50 m s^{-1}.

In our coupled simulation of the Late Ordovician glaciation, strong katabatic winds begin to form as the ice sheet grows (Fig. 4e-h). When there is no ice sheet, the cold polar air mainly blows towards the ocean between 90° W and 0° E (Fig. 4a-d), especially in the austral winter, while warm air blows polewards in the summer at certain locations on the continents (e.g. between 135° W and 180° W). This warm air advection will prevent ice sheet from growing in the offline simulation. In the coupled simulation, however, once an ice sheet is present, the cold air blows towards the continental interior in both winter and summer, expanding the low-temperature (<0 °C) region (compare Fig. 4e,i to 4a). Ice-sheet formation thus leads to a fundamental reorganization of regional atmospheric circulation, marked by the development of strong katabatic winds. Cooling and densification of air over the cold ice-sheet surface allow dense air to drain downslope from the ice-sheet interior toward surrounding lowland area, generating cold, gravity-driven near-surface flows. This enhanced cold air helps increase snow accumulation during winter and spring, and reduce ablation during summer around the ice sheet's edges.

https://doi.org/10.5194/egusphere-2026-1385
Preprint. Discussion started: 19 March 2026

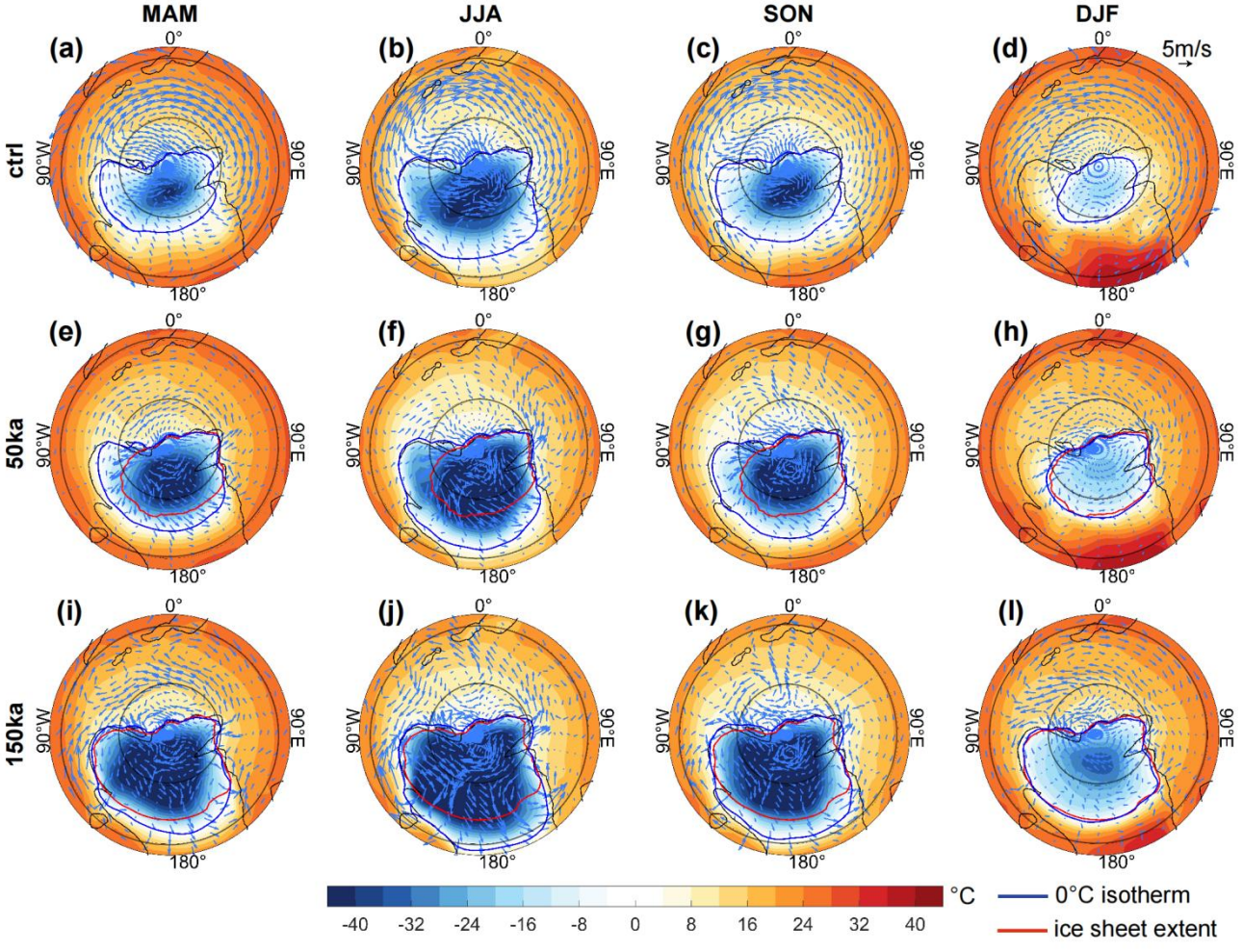

Figure 4: Surface wind field and temperature. (a-d) Surface wind field and surface temperature from the equilibrium of the control experiment for March, April, May (MAM); austral winter (June, July, and August; JJA); September, October, November (SON); and austral summer (December, January, and February; DJF). Two snapshots from the coupled framework simulation are shown in **(e-h)** 50 ka, **(i-l)** 150 ka. Note that in (e-h) and (i-l), the surface wind is shown as the difference from the control run. The 0 °C isotherm and ice-sheet extent are indicated by the black and red contours, respectively. Latitude is shown at 30° intervals.

When the ice sheet expands to ~42° S (red curves in Fig. 4i-l), the katabatic remains strong in austral winter, but becomes negligible or even reverses its direction in summer. That is, warm air starts to blow towards the ice sheet, increasing ablation and preventing the ice sheet from further expanding. This seasonal asymmetry reflects a fundamental shift in the near-surface thermal and dynamical controls on the flows. During summer, increased solar heating warms the mid-latitude ice-sheet surface and the overlying boundary-layer air, eroding the strong surface cooling that drives cold air downslope drainage. As a result, the gravity driven cold air advection along the ice-sheet slopes is greatly reduced in austral summer. And as the ice sheet expands, the ice front reaches sufficiently low latitudes, where the surface temperatures sustain high ablation rates. Under such conditions, the enhanced melt counteracts further margin advance, consistent with the negative

https://doi.org/10.5194/egusphere-2026-1385
Preprint. Discussion started: 19 March 2026

feedback mechanism described earlier, in which ice-sheet expansion into ablation-prone zones can offset mass gain and finally stabilize the ice sheet. This result highlights the positive feedback mechanism of "ice sheet growth-katabatic winds of cold air advection-continued ice sheet growth" during the Late Ordovician, providing a clear dynamic explanation for the rapid expansion of the ice sheet during this period.

3.4 Equilibrium climate change due to ice sheet

Figure 5 shows the surface temperature from both the control (offline experiment) and coupled experiments, along with the differences between the coupled run relative to the control. In the control experiment, the land (mostly bare; Fig. 2a) is much colder than the oceans during the austral winter (Fig. 5a) partially because of the presence of snow and associated high surface albedo (not shown). The seasonal cycle of the surface temperature over land is much stronger than over oceans (compare Figs. 5b and 5a). Because the majority landmass was located in the mid- to high-latitude region of the SH, this hemisphere exhibits stronger seasonal variations and colder annual mean surface temperature than the Northern Hemisphere (NH).

https://doi.org/10.5194/egusphere-2026-1385
Preprint. Discussion started: 19 March 2026

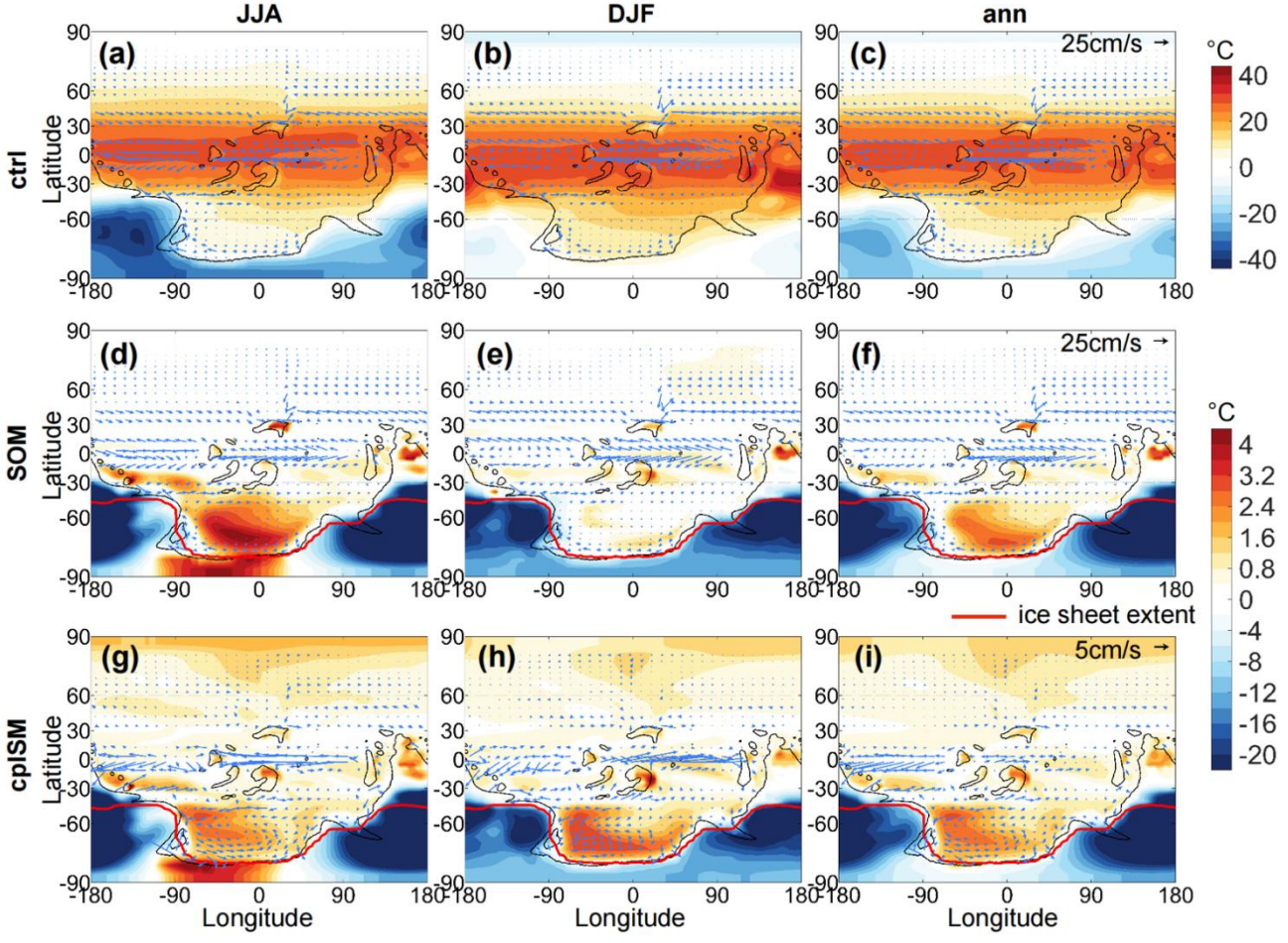

Figure 5: Surface temperature and ocean surface currents. (a-c) Surface temperature and ocean surface currents (averaged over the upper 50m) from the control experiment for austral summer (DJF), winter (JJA), and annual means. **(d-f)** Temperature differences between the SOM experiment and the control experiment, with the ocean currents of the control experiments superimposed. **(g-i)** The difference in surface temperature and ocean surface currents between the fully coupled experiment and the control experiment. Note that the color scale is different when showing positive and negative temperature differences.

Surprisingly, surface temperature increases in many regions when a large ice sheet grows. These regions include tropical lands, the global ocean, and even the ice sheet in a small region around the South Pole (Fig. 5g-i). The increase in local temperature can exceed 4 °C in some areas. The results of SOM experiments (and prescribed-SST experiments as will be shown later) indicate that the SH ocean warming as well as the warming over tropical lands is primarily driven by atmospheric processes (Fig. 5d-f), while the NH ocean warming is mainly triggered by oceanic processes (compare Fig. 5g-i to 5d-f).

The warming over the high-latitude SH ocean is due to the strengthening of a stationary wave between 30° S-60° S when a large ice sheet develops. This stationary wave has a wavenumber-1 structure as evidenced by the 500 hPa eddy geopotential

https://doi.org/10.5194/egusphere-2026-1385
Preprint. Discussion started: 19 March 2026

height field (Fig. 6). In the control, where only a small ice sheet exists (Fig. 2a) along the mountain range (Fig. 1), the high- and low-pressure anomalies are located over the windward and leeward sides of mountain range, respectively (Fig. 6a-c), very similar to what happens near the Rockies and Tibetan Plateau of the present day (Held et al., 2002; Lee et al., 2023). The two nodal points—pressure anomalies are zero—are located at the middle of ocean and continent, respectively. The one at the middle of the ocean guides warm low-latitude air into the high-latitude region, while the one at the middle of continent guides cold high-latitude air into the low-latitude region.

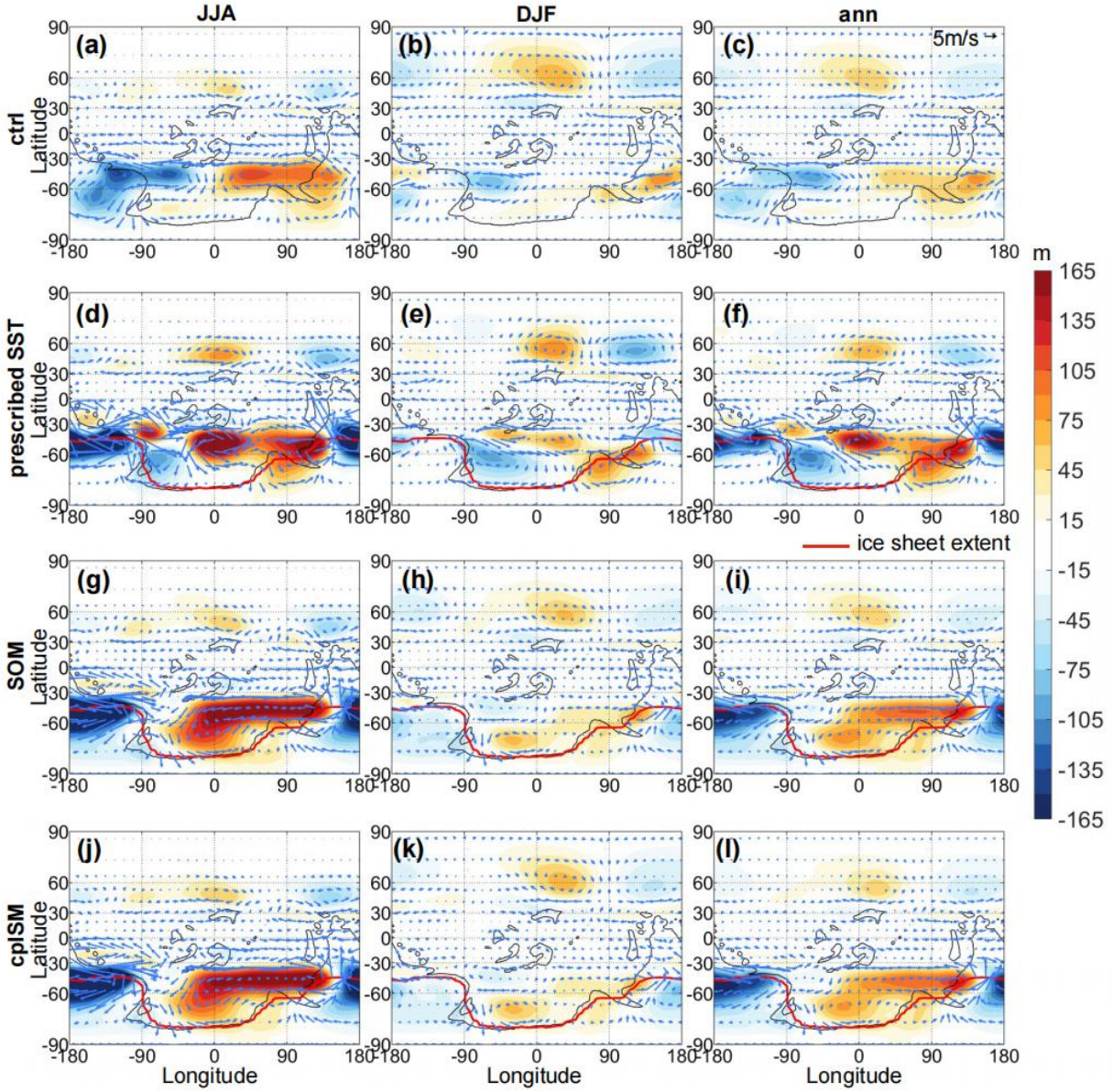

https://doi.org/10.5194/egusphere-2026-1385
Preprint. Discussion started: 19 March 2026

Figure 6: Structure of the stationary waves. (a-c) 500 hPa geopotential height and wind field from the control experiment, with zonal average subtracted. **(d-f)** As **(a-c)**, but for the prescribed-SST experiment results. And **(g-i)** for the SOM experiment, **(j-l)** for the coupled experiment.

When a large ice sheet develops on the continent, the SH stationary wave is substantially strengthened (Fig. 6d-l), especially during the austral winter, enhancing atmospheric heat transport towards the high latitude over the ocean region (Fig. 7). This strengthening happens in the prescribed-SST experiment (Fig. 6d-f), indicating a primary influence of the ice sheet on the atmospheric circulation. Along with the strengthening, the phase of the stationary wave shift westwards by about 30° longitude. Both the strengthening and westward shift of the wave are likely due to the enhanced blocking of the westerly wind by the high topography of ice sheet and the westward shift of ice edges (compare Fig. 2a and 2b). The southward transport of warm air with a temperature anomaly of 3-4 °C across 65° S at the nodal point (~60° W) is clearly demonstrated in Fig. 7.

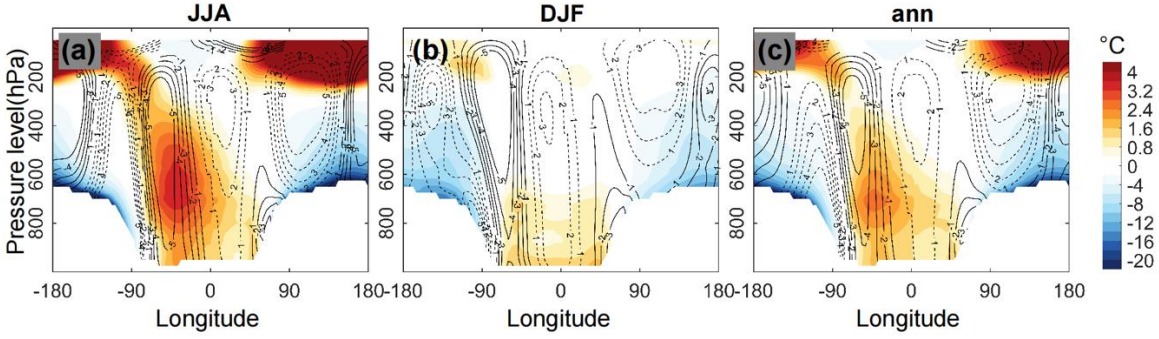

Figure 7: Difference in air temperature (color shading) and meridional wind (contours) along 65° S between the coupled and the control experiments. Solid and dashed contours indicate northerly and southerly wind anomalies, respectively. Note that the color scale is different when showing positive and negative temperature differences.

When the SST is allowed to change (as in the SOM simulation), the pattern of this stationary wave is slightly modified and extends more poleward (compare Fig. 6d-f to 6g-i), enabling atmospheric heat transport towards even higher latitude. Note that sea ice plays a negligible role in this change because it is nearly absent even during the austral winter. This pattern remains almost the same when the ocean dynamics are turned on (as in the coupled ice-climate simulation; compare Fig. 6g-i to 6j-l) but the surface ocean current also help transport more heat to the high-latitude region (Fig. 5g-i). Due to the strengthening of the high-pressure anomaly over the oceanic region, the clouds and the associated negative radiative forcing are reduced (Fig. 8d-f; the net effect of reduced shortwave cloud radiative forcing results in net energy gain at the surface), also having a warming effect. In any case, the results highlight the importance of the atmospheric process in driving the warming over the mid- to high-latitude oceanic region.

https://doi.org/10.5194/egusphere-2026-1385
Preprint. Discussion started: 19 March 2026

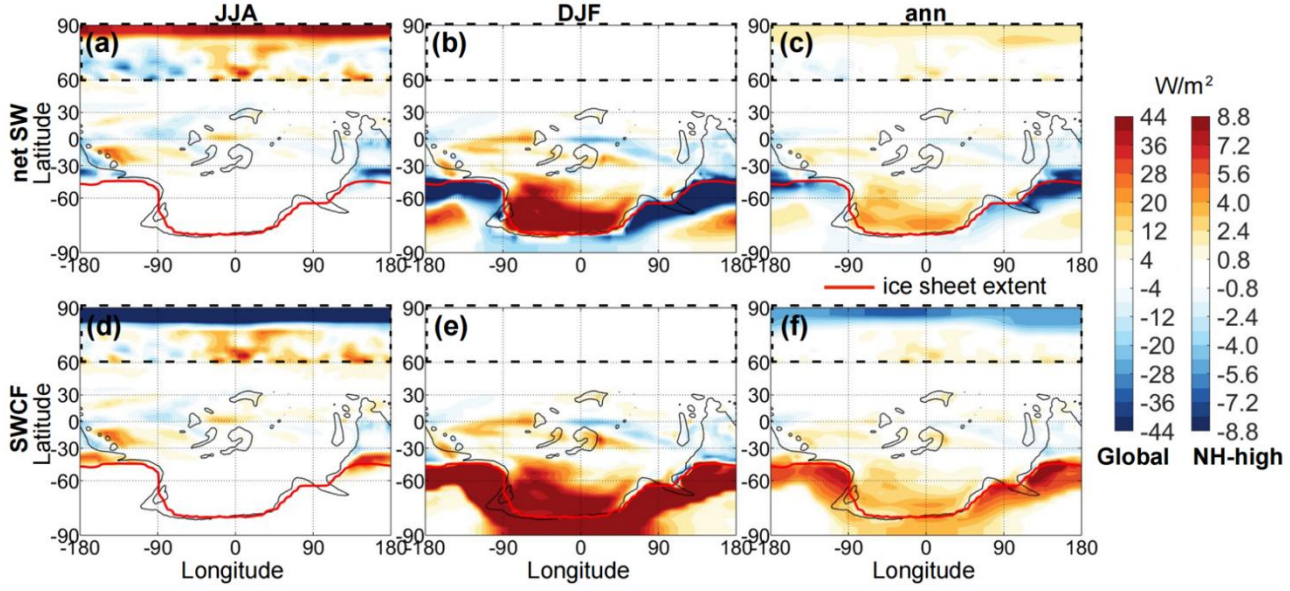

Figure 8: The differences in (a-c) net surface radiation and (d-f) shortwave cloud radiative forcing between the coupled and the control experiments. The net surface radiation includes both the shortwave and longwave radiation, with downward being positive. Note that the color range for high latitudes in the NH (black dashed box) has been adjusted, as the radiation changes in the NH are relatively minor.

The warming over different tropical lands in the coupled simulations relative to the control are due to different reasons. For islands, the primary reason is the reduced clouds and associated blocking effect to solar radiation (Fig. 8). While for the tail of the supercontinent extruding into the tropical region, the warming is caused by the enhanced easterly winds (Fig. 6d-f) which brings air from the warmer adjacent ocean (Fig. 5a-c) to the continent.

The NH warming does not appear in the SOM simulation, indicating a primary role of the ocean dynamics. The changes in both the deep meridional overturning circulation (MOC) and the subtropical cell (STC) could play a role. As the SH polar ocean warms, the deepwater formation there weakens, so does the MOC (Fig. 9). In the meantime, the STC of the SH becomes shallower (Fig. 9). The weakening of this anti-clockwise MOC and shallowing of STC should reduce the southward heat transport across the equator and warm the NH.

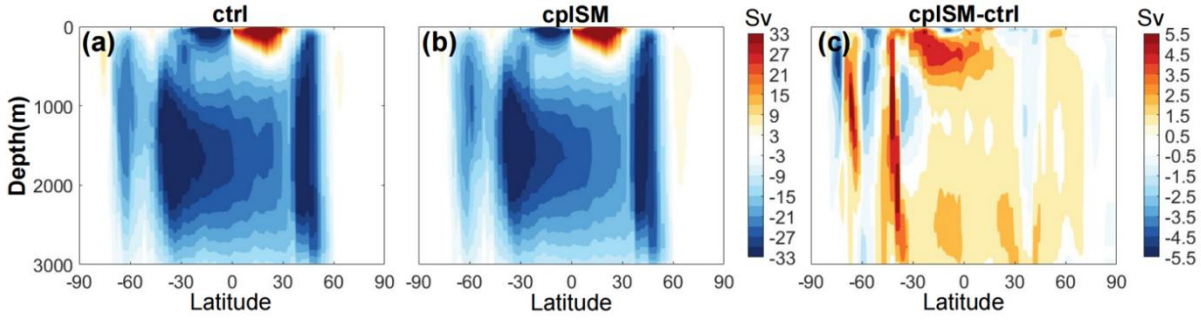

https://doi.org/10.5194/egusphere-2026-1385
Preprint. Discussion started: 19 March 2026

Figure 9: Oceanic meridional overturning circulation. Panels show the ocean meridional overturning streamfunction for **(a)** Control simulation, **(b)** Coupled simulation and **(c)** the difference (Coupled minus Control). Negative values indicate counterclockwise circulation.

The change of oceanic heat transport confirms that less (~0.08 PW; 1 PW = 1015 Watts) heat is transported southward across the equator and more heat is transported towards the NH by the ocean when a large ice sheet develops (blue curves in Fig. 10). While the atmospheric heat transport remains almost the same at the equator (red curves in Fig. 10), making the total heat transport (black curves in Fig. 10) towards the NH increase. Note that the oceanic and total heat transport towards the NH high-latitude region decreases in the ice sheet-climate coupled simulation compared with the control simulation. This is because the results shown in Fig. 10 are for the equilibrium states, at which the NH polar region has already warmed (Fig. 5g-i). At the beginning of the coupled simulation, the oceanic heat transport does increase in the NH high latitudes, reducing the sea ice there. In the latter stage, the reduced sea ice (not shown) and thus increased absorption of solar radiation (Fig. 8) sustain the warming there.

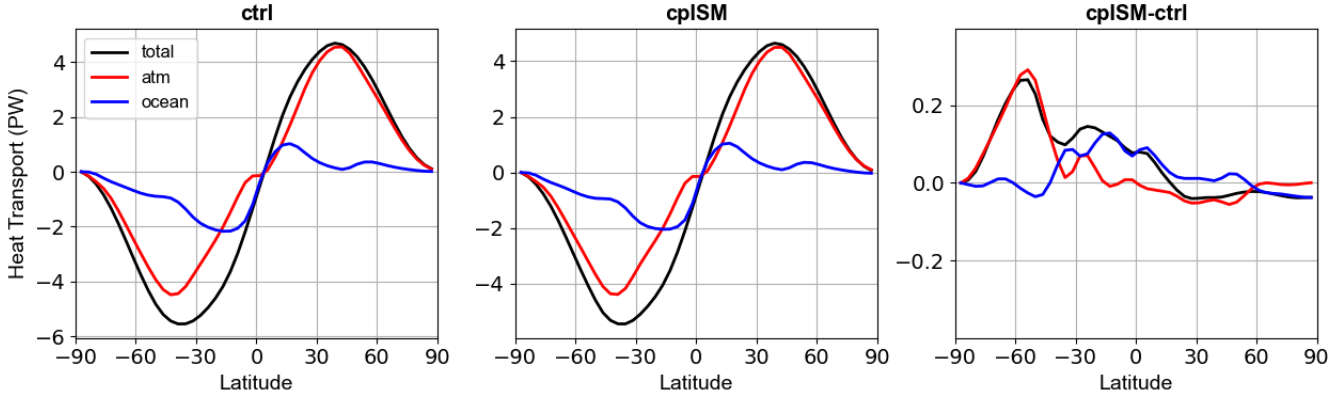

Figure 10: Simulated meridional heat transport. Panels show the total, atmospheric, and oceanic contributions to the meridional heat transport. **(a)** Control simulation, **(b)** Coupled simulation and **(c)** the difference (Coupled minus Control). Positive values indicate northward heat transport.

3.5 Implication to the duration of the Ordovician continental ice sheet

One unresolved question concerns the precise time of continental ice sheet initiation and persistence during the Ordovician cooling interval. Trotter et al. (2008) used oxygen isotope ($\delta^{18}O$) data to outline the long-term climate evolution during the Ordovician (Fig. B4), identifying a transition from greenhouse conditions (~42 °C at palaeoequator) to near-modern equatorial temperatures (~28 °C) along with a rapid cooling episode during the Hirnantian. Conventional interpretations have generally suggested that mid-latitude continental ice sheets were short-lived (~1 Ma) (Bergmann et al., 2025; Cocks and Torsvik, 2021; Delabroye and Vecoli, 2010; Finnegan et al., 2011), appearing only briefly during the Hirnantian. In contrast, Finnegan et al. (2011) used clumped-isotope data to argue for substantial land-based ice volumes well before the Hirnantian, potentially as early as the Katian. Furthermore, Pohl et al. (2016) provided support from coupled ice-sheet modelling simulations for a prolonged glaciation that may have begun as early as the Middle Ordovician.

https://doi.org/10.5194/egusphere-2026-1385
Preprint. Discussion started: 19 March 2026

Our simulations show that the initial formation and early expansion of the ice sheet have minimal impact on tropical SSTs, suggesting that the ice sheet activity may not be accompanied by global-scale cooling. On the contrary, the appearance of a large ice sheet plays a crucial role in maintaining ocean temperature stability, delaying its sharp cooling. This implies that the tropical oxygen isotopes, such as those from Trotter et al. (2008), are unlikely to record major temperature shifts at high latitudes. Based on a comparison with the tropical SSTs in our coupled simulations and records, the equatorial temperatures of such condition in our model work (a large continental ice sheet in 6 PAL) may correspond more to the Middle Ordovician. This finding corroborates the emerging theory that a large ice sheet was not only widespread during the Hirnantian (~443 Ma), but could have covered much of the Gondwana supercontinent during the Middle and Late Ordovician (470-440 Ma), supporting the "early Palaeozoic Ice Age" paradigm.

4 Conclusions

To assess the critical role of ice sheet-climate interactions in Late Ordovician glaciation, this study conducted both uncoupled and coupled simulation experiments. The results indicate that the inclusion of bidirectional feedback between the ice sheets and the climate system is a key factor in determining the realism of the simulation outcomes. For pCO2 (= 6 PAL) suitable for obtaining GMST that is consistent with reconstruction, the uncoupled model obtains an ice sheet confined to the polar regions (≥60° S), contradicting the geological records. In contrast, the coupled model is able to simulate a large ice sheet that covers the southern part of Gondwana, extending to about 40° S. The coupled simulation shows that the growth of the Late Ordovician Gondwana ice sheet was mainly controlled by the ablation process, rather than accumulation. We identify a key positive feedback, that is, the "ice sheet growth- cold air advection due to katabatic winds-further ice sheet expansion" feedback, which provides a crucial mechanism for the substantial expansion of the ice sheet during the Late Ordovician. Furthermore, no large-scale sea ice was observed in the simulation, indicating that sea ice formation was more difficult than land ice formation under these conditions.

Although the expansion of ice sheet in this time period induced cooling over the mid- to high-latitude continental region, it induced warming over all the other regions, especially over the high-latitude oceans. This warming was initiated in the SH by the enhanced poleward atmospheric heat transport, which itself was due to the enhanced wavenumber-1 stationary wave by the expansion of ice sheet. This warming was then amplified by reduction of clouds and the warming pattern adjusted by the oceanic heat transport. This warming then weakened the deepwater formation in the SH polar region and thus the MOC, which originally acted to transport heat from the NH to SH. The weakening of this MOC increased the northward heat transport across the equator, which reduced sea ice in the NH polar region. This latter process is eventually responsible for the warming of the NH polar region. These results highlight the complex and unintuitive repones of the surface temperature, oceanic, and atmospheric responses to ice-sheet expansion during the Late Ordovician.

Our simulation results suggest that the appearance of a large ice sheet warms the ocean, implying that the tropical oxygen isotopes, such as those from Trotter et al. (2008), might not record major temperature shifts at high latitudes. Our results thus

https://doi.org/10.5194/egusphere-2026-1385
Preprint. Discussion started: 19 March 2026

suggest that the "early Palaeozoic Ice Age" paradigm is not inconsistent with reconstructions, that is, a large ice sheet was not only widespread during the Hirnantian (~443 Ma), but could have covered much of the Gondwana supercontinent during the Middle and Late Ordovician (470-440 Ma).

Although this study highlights the critical role of ice sheet-climate feedback, there are several limitations. First, the treatment of orbital forcing in this study is simple, and a more realistic representation of orbital variations should be considered in future work. Second, this study primarily focuses on the interactions between the atmosphere and ice sheets, and does not fully explore the potential impacts of sea level drop. Additionally, the influence of dust, which could be much heavier than today (Liu et al., 2020), was not considered. Future studies that incorporate more detailed Earth system processes will likely provide a more comprehensive understanding of the underlying mechanisms driving the Late Ordovician glaciation and associated biological events.

Appendix A: SMB calculation in the ice sheet model (ISSM)

The simulations of continental ice sheets were performed using the Ice-sheet and Sea-level System Model version 4.23 (ISSM 4.23), jointly developed by NASA Jet Propulsion Laboratory (JPL) and the University of California, Irvine (UCI). ISSM is a finite-element, thermo-mechanically coupled ice sheet model that solves the mass, momentum, and energy balance equations on an unstructured mesh. In this study, the model is configured at a horizontal resolution of 60 km with 15 vertical levels, and the dynamical core is based on the Shallow Ice Approximation (SIA). The basal melt rate beneath floating ice shelves is prescribed as 0.1 m yr^{-1}, within the range commonly adopted in previous Antarctic ice sheet studies.

ISSM uses monthly mean surface temperature and precipitation from the CESM simulations to calculate surface mass balance. Surface accumulation is directly derived from the frozen fraction of precipitation, while ablation is calculated using the Positive Degree-Day (PDD) method, and superimposed ice formation is represented by a parameterization scheme.

Here, the model calculates surface accumulation using monthly mean surface temperature and precipitation. When temperatures are below 0 °C, precipitation is treated as snowfall. A normal distribution of the hourly temperature is also assumed to compute the amount of snow accumulation from the precipitation. A lower standard deviation $\sigma_{RS} = \sigma_{PDD} - 0.5$ is assumed in that case to take into account the smaller temperature variability during cloudy days.

$$\frac{accumulation}{precipitation} = \frac{\rho_i}{\rho_w \sigma_{RS}\sqrt{2\pi}} \int_0^{1year} \int_{T_m-2.5\sigma_{RS}}^{0°C} exp\left[\frac{-(T-T_m)^2}{2\sigma_{RS}^2}\right] dTdt \qquad (1)$$

Melting is calculated using the PDD method based on temperature and precipitation fields. In all PDD-based calculations, the mean value is the monthly average temperature (T_m) and a standard deviation (σ_{PDD}) of 5.5 °C is applied to account for monthly air temperature variability. The number of days for which the temperature is above 0 °C in a year is computed as follows:

$$\mathrm{PDD} = \frac{1}{\sigma_{PDD}\sqrt{2\pi}} \int_0^{1year} \int_{0°C}^{T_m+2.5\sigma_{PDD}} T exp\left[\frac{-(T-T_m)^2}{2\sigma_{PDD}^2}\right] dTdt \qquad (2)$$

https://doi.org/10.5194/egusphere-2026-1385
Preprint. Discussion started: 19 March 2026

The PDD approach assumes that near-surface air temperature controls melt processes through an empirical relationship with the melting point. Despite its simplicity, this scheme has been demonstrated to reproduce large-scale ice sheet behavior effectively and efficiently.

The amount of snow and ice melts is directly proportional to the number of positive degree days. Snow melts first, with the remaining positive degree days used to melt ice. By incorporating a dependency on the average summer temperature, the ablation rate factors for snow (γ_{snow}) and ice (γ_{ice}) can be calculated:

$$\gamma_{ice} = \begin{cases} 17.22mm/PDD; T_{summer} \leq -1℃ \\ 0.0067 \times (10 - T_{summer})^3 + 8.3mm/PDD; -1\ ℃ < T_{summer} < 10℃ \\ 8.3mm/PDD; 10\ ℃ \leq T_{summer} \end{cases} \quad (3)$$

and

$$\gamma_{snow} = \begin{cases} 2.65mm/PDD; T_{summer} \leq -1℃ \\ 0.15 \times T_{summer} + 2.8mm/PDD; -1\ ℃ < T_{summer} < 10℃ \\ 4.3mm/PDD; 10\ ℃ \leq T_{summer} \end{cases} \quad (4)$$

A fraction of the melted snow is refrozen. The amount of ice that refreezes within a year is:

$$\text{superimposed ice} = \begin{cases} min[Pr + M, 2.2 \times (Ps - M) - d \times ci/L \times min(Tsurf, 0\ ℃)]; M \leq Ps \\ min[Pr + M, d \times ci/L \times min(Tsurf, 0\ ℃)]; M > Ps \end{cases} \quad (5)$$

Where， Pr is the rainfall in a year ， Ps is the snow fall in a year， M is the snow melt in a year， d is the active thermodynamic layer (set to 1 m)， ci is the ice specific heat capacity (152.5 + 7.122T J kg^{-1} K^{-1})， L is the latent heat fusion (3.35×105 J kg^{-1})， $Tsurf$ is the surface temperature.

For the basal friction formulation, the Paterson-type sliding law is employed, with parameter values calibrated to best reproduce modern Antarctic ice volume and flow patterns.

https://doi.org/10.5194/egusphere-2026-1385
Preprint. Discussion started: 19 March 2026

Appendix B: supplementary figures

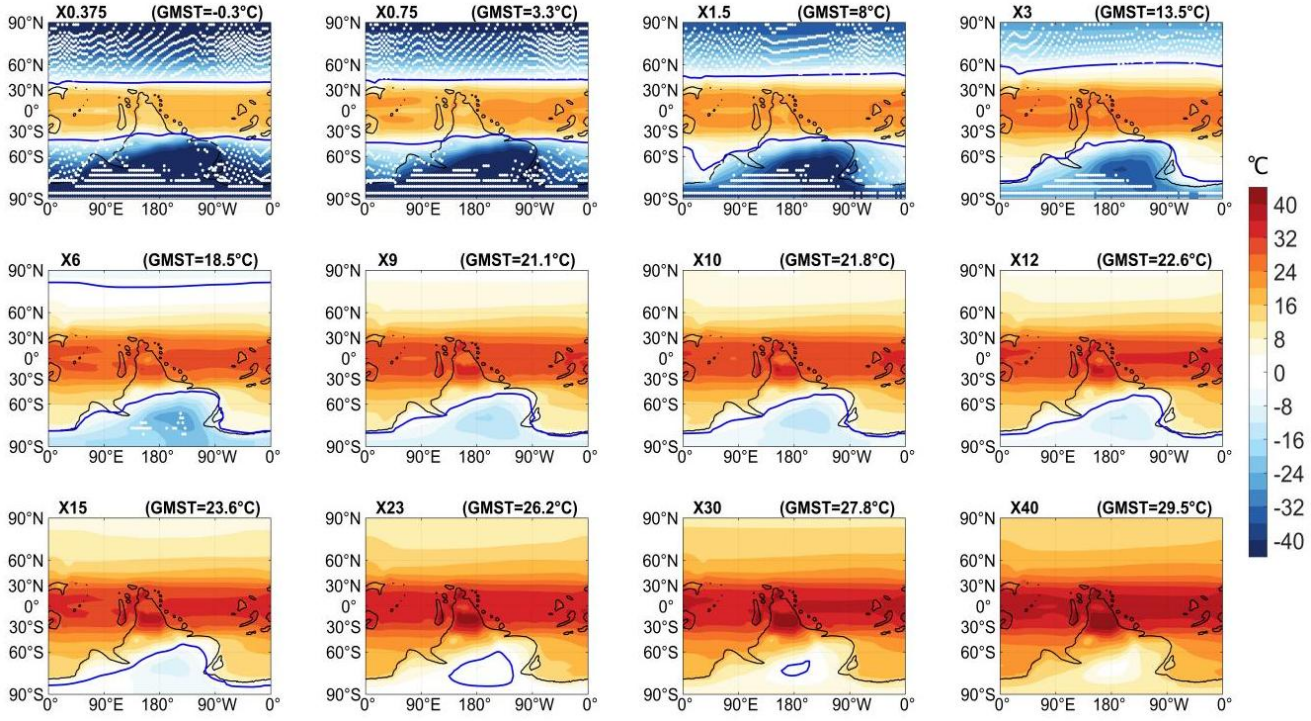

Figure B1: Late Ordovician climate sensitivity to CO_2. Annual mean surface temperature under different PAL CO_2 conditions. White dots represent the extent of the cryosphere: sea ice is defined based on the annual mean sea ice fraction (indicating perennial ice), while land ice is defined as areas where the annual mean water-equivalent snow depth exceeds 1 m, representing potential regions for continental ice development. The results show that, in the uncoupled ice sheet scenario, a CO_2 level of 6 PAL marks the threshold for initiating continental ice formation, whereas only when greenhouse gas concentrations drop sufficiently low (~1 PAL) can land ice marginally extend to around 60° S. The development of sea ice in the SH ocean lags that of land ice. The blue solid lines represent the 0 °C.

https://doi.org/10.5194/egusphere-2026-1385
Preprint. Discussion started: 19 March 2026

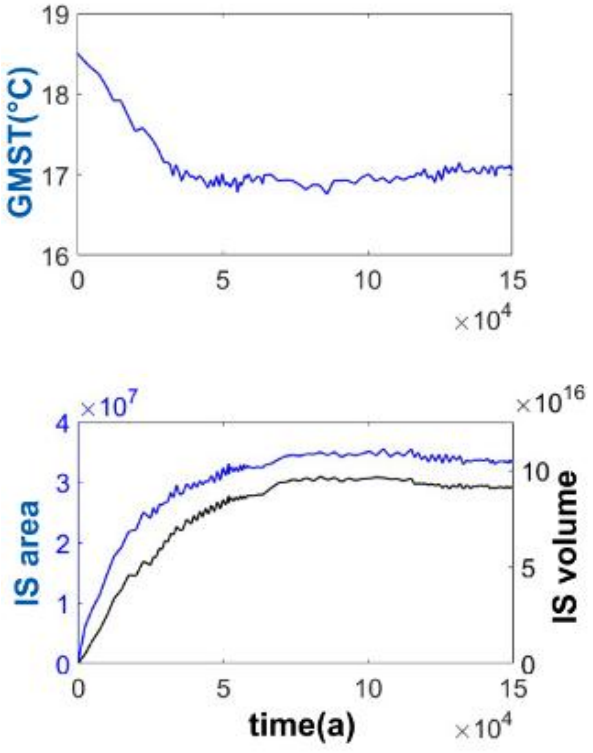

Figure B2: Ice Sheet Coupled Time Series. Time series of temperature, area(m^2), and volume(m^3) for ice sheet coupling

https://doi.org/10.5194/egusphere-2026-1385
Preprint. Discussion started: 19 March 2026

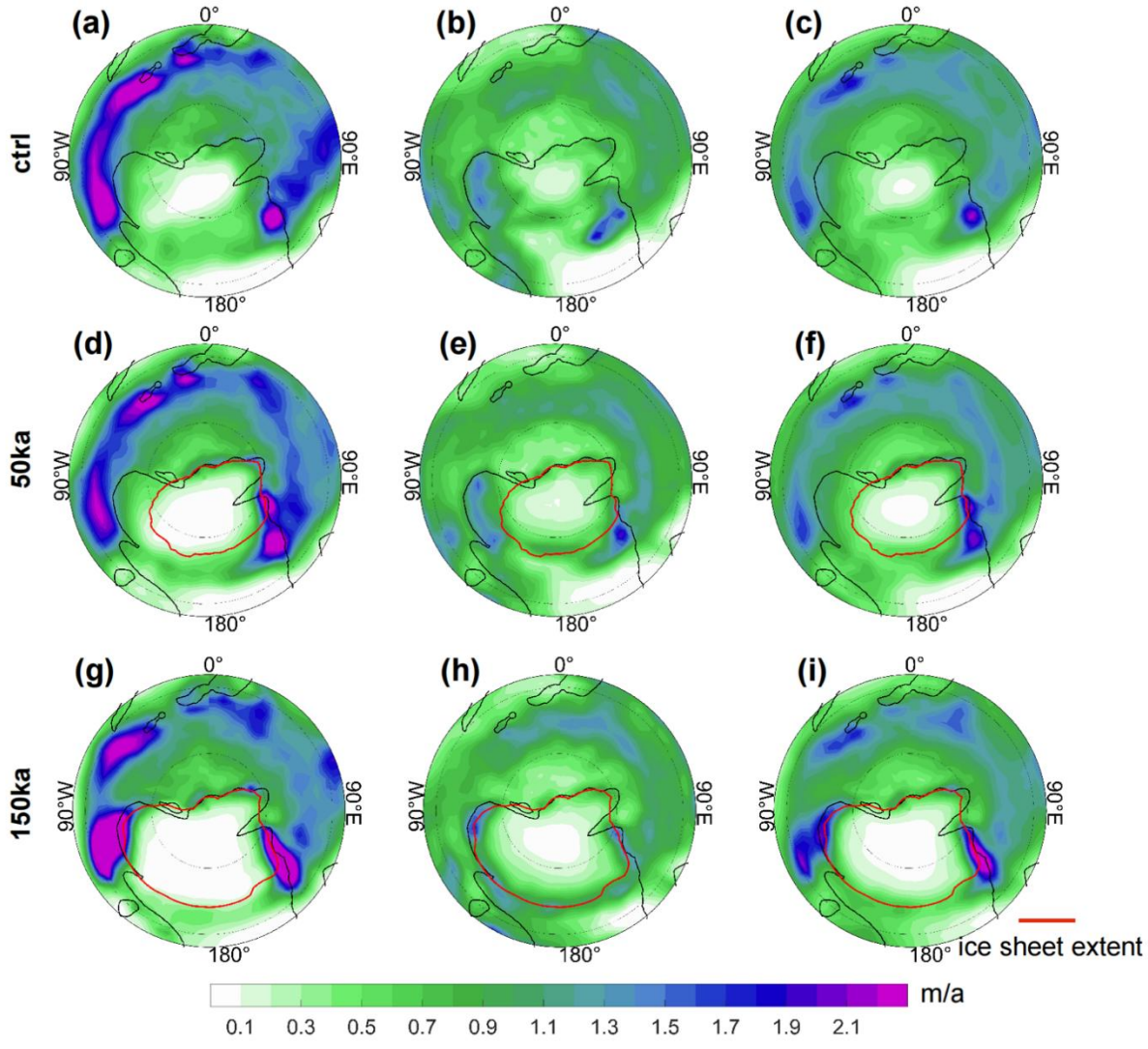

Figure B3: Evolution of precipitation fields. (a-c) Precipitation fields for the control experiment. Two snapshots for the coupled run: **(d-f)** 50 ka, **(g-i)** 150 ka (equilibrium state).

https://doi.org/10.5194/egusphere-2026-1385
Preprint. Discussion started: 19 March 2026

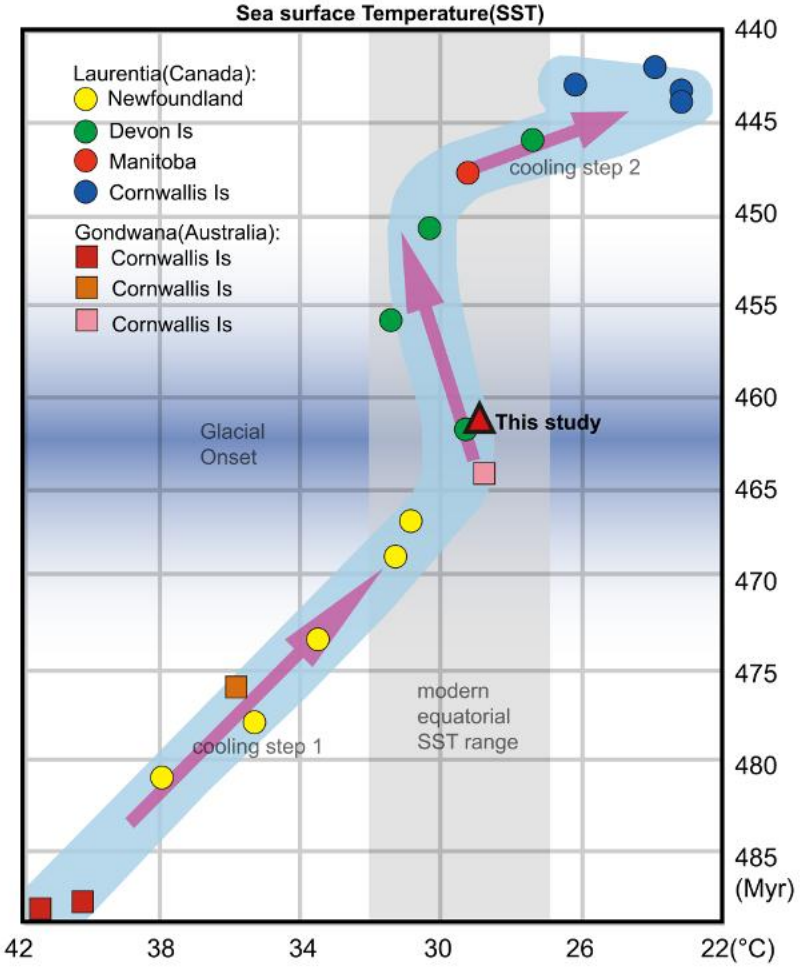

460 **Figure B4: Tropical seawater temperature trend.** Generalized tropical seawater temperature trend throughout the Ordovician, derived from conodont oxygen isotope compositions measured in situ. Temperature means are plotted for different analytical sessions. The blue line represents the primary first-order temporal trend of Ordovician sea-surface temperatures. The red triangles represent the tropical sea surface temperatures from this study. Note that these temperatures do not correspond directly in time but have been placed at the Mid-Ordovician based on corresponding temperatures. (Adapted from Trotter et al., 2008)

https://doi.org/10.5194/egusphere-2026-1385
Preprint. Discussion started: 19 March 2026

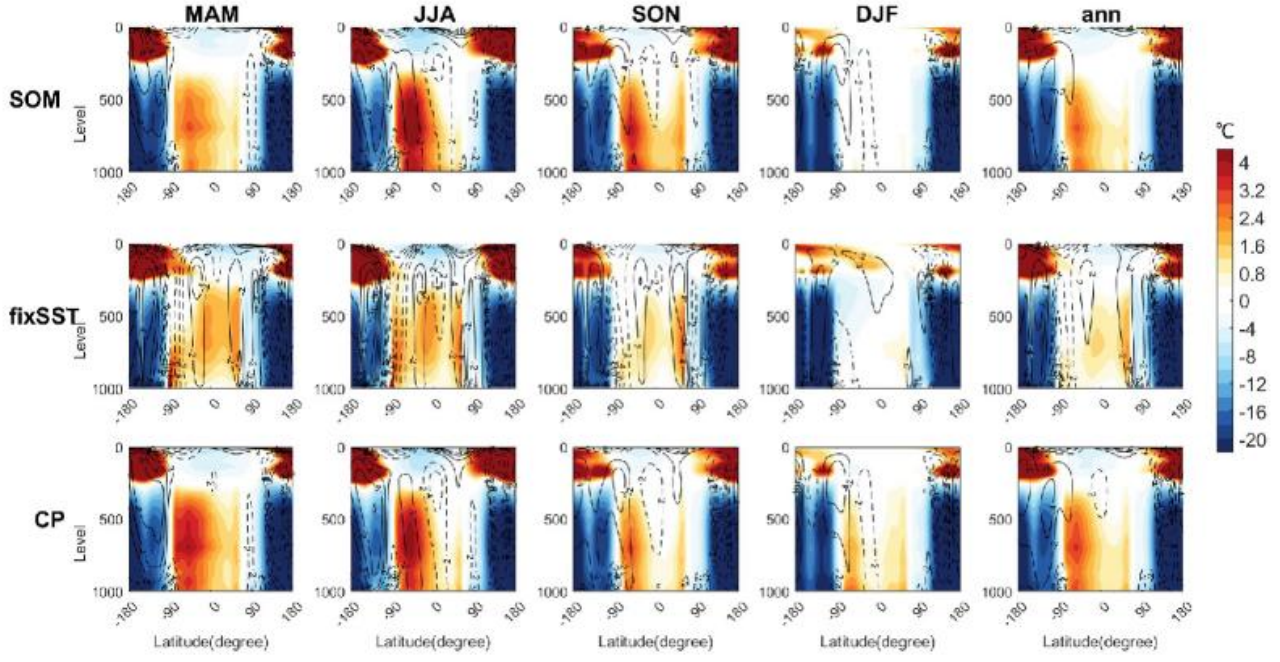

Figure B5: 65° S profile. 65° S profile, with shaded areas representing temperature and contour lines representing meridional wind. Solid lines indicate northerly winds, and dashed lines indicate southerly winds. Note that the color scale is uneven when showing temperature differences, while the warming section has been artificially amplified. Time average for March, April, May (MAM); austral winter (June, July, and August, JJA); September, October, November (SON); austral summer (December, January, and February, DJF) and annual means. SOM: Slab Ocean Mod; fixSST: Prescribed SST; CP: Coupled.

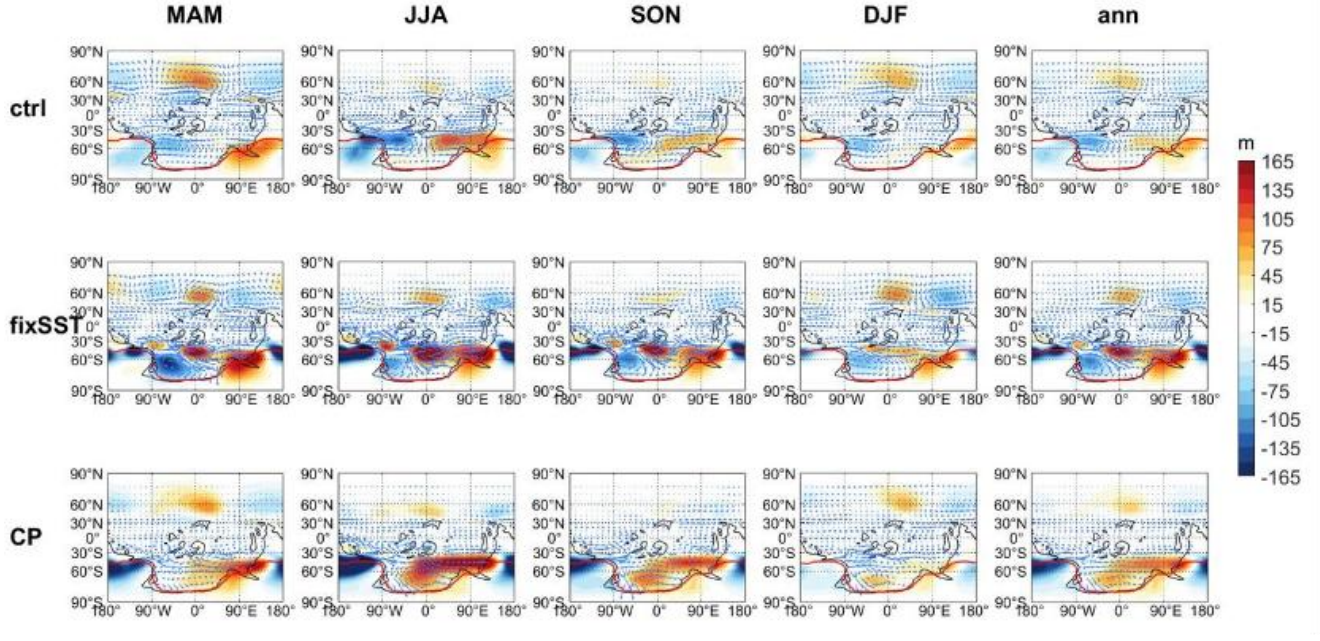

https://doi.org/10.5194/egusphere-2026-1385
Preprint. Discussion started: 19 March 2026

Figure B6: Stationary waves structure of the prescribed SST experiment. 500 hPa geopotential height and wind field from the control experiment, with zonal average subtracted. Top row: Control experiment. Middle row: Prescribed SST experiment. Bottom row: Coupled experiment.

Code, data, or code and data availability

CESM 1.2.2 (https://www2.cesm.ucar.edu/models/cesm1.2/) and ISSM (https://issm.jpl.nasa.gov/) are open-source software. Simulation results can be retrieved from https://doi.org/10.18170/DVN/8XRV32.

Author contributions

Yongyun Hu and Yonggang Liu contributed to the conceptualization and initiation of this work and provided advice and direction in the analysis of results. Yudong Sun and Yonggang Liu co-designed and co-wrote the paper, with Yudong Sun conducting the model simulation and leading the figure generation. Qiang Wei and Jiacheng Wu assisted in designing the coupled framework. All authors contributed to the development and revision of the article. The final presentation of the published work, specifically the initial draft, was prepared by Yudong Sun.

Competing interests

The contact author has declared that none of the authors has any competing interests.

Acknowledgements

We acknowledge Lei Wang from Fudan University for discussions on the Southern Hemispheric stationary waves.

Financial support

This work is supported by the National Natural Science Foundation of China (42488201; 42225606) and the National Key R&D Program of China (2023YFF0805200). Simulations are conducted at the High-performance Computing Platform of Peking University.

Review statement

The review statement will be added by Copernicus Publications listing the handling editor as well as all contributing referees according to their status anonymous or identified.

https://doi.org/10.5194/egusphere-2026-1385
Preprint. Discussion started: 19 March 2026

References

Bergmann, K. D., Macdonald, F. A., and Swanson-Hysell, N. L.: The Causes and Consequences of Ordovician Cooling, Annual Review of Earth and Planetary Sciences, https://doi.org/10.1146/annurev-earth-040523-114630, 2025.

Berner, R. A.: GEOCARB II; a revised model of atmospheric CO_2 over Phanerozoic time, American Journal of Science, 294, 56–91, https://doi.org/10.2475/ajs.294.1.56, 1994.

Caputo, M. and Crowell, J.: Migration of glacial centers across Gondwana during Paleozoic Era, Geological Society of America Bulletin, 96, 1985.

Cocks, L. R. M. and Torsvik, T. H.: Ordovician palaeogeography and climate change, Gondwana Research, 100, 53–72, https://doi.org/10.1016/j.gr.2020.09.008, 2021.

Connolley, W. M.: The Antarctic Temperature Inversion, International Journal of Climatology, 16, 1333–1342, https://doi.org/10.1002/(SICI)1097-0088(199612)16:12<1333::AID-JOC96>3.0.CO;2-6, 1996.

Crowley, T. J. and Baum, S. K.: Toward reconciliation of Late Ordovician (~440 Ma) glaciation with very high CO_2 levels, Journal of Geophysical Research: Atmospheres, 96, 22597–22610, https://doi.org/10.1029/91JD02449, 1991.

Crowley, T. J. and Baum, S. K.: Reconciling Late Ordovician (440 Ma) glaciation with very high (14X) CO_2 levels, Journal of Geophysical Research: Atmospheres, 100, 1093–1101, https://doi.org/10.1029/94JD02521, 1995.

Crowley, T. J., Mengel, J. G., and Short, D. A.: Gondwanaland's seasonal cycle, Nature, 329, 803–807, https://doi.org/10.1038/329803a0, 1987.

Delabroye, A. and Vecoli, M.: The end-Ordovician glaciation and the Hirnantian Stage: A global review and questions about Late Ordovician event stratigraphy, Earth-Science Reviews, 98, 269–282, https://doi.org/10.1016/j.earscirev.2009.10.010, 2010.

Finnegan, S., Bergmann, K., Eiler, J. M., Jones, D. S., Fike, D. A., Eisenman, I., Hughes, N. C., Tripati, A. K., and Fischer, W. W.: The Magnitude and Duration of Late Ordovician–Early Silurian Glaciation, Science, 331, 903–906, https://doi.org/10.1126/science.1200803, 2011.

Fyke, J., Sergienko, O., Löfverström, M., Price, S., and Lenaerts, J. T. M.: An Overview of Interactions and Feedbacks Between Ice Sheets and the Earth System, Reviews of Geophysics, 56, 361–408, https://doi.org/10.1029/2018RG000600, 2018.

Gong, X., Zhang, X., Lohmann, G., Wei, W., Zhang, X., and Pfeiffer, M.: Higher Laurentide and Greenland ice sheets strengthen the North Atlantic ocean circulation, Clim Dyn, 45, 139–150, https://doi.org/10.1007/s00382-015-2502-8, 2015.

Gregoire, L. J., Otto-Bliesner, B., Valdes, P. J., and Ivanovic, R.: Abrupt Bølling warming and ice saddle collapse contributions to the Meltwater Pulse 1a rapid sea level rise, Geophysical Research Letters, 43, 9130–9137, https://doi.org/10.1002/2016GL070356, 2016.

Gregoire, L. J., Ivanovic, R. F., Maycock, A. C., Valdes, P. J., and Stevenson, S.: Holocene lowering of the Laurentide ice sheet affects North Atlantic gyre circulation and climate, Clim Dyn, 51, 3797–3813, https://doi.org/10.1007/s00382-018-4111-9, 2018.

Hakuba, M. Z., Folini, D., Wild, M., and Schär, C.: Impact of Greenland's topographic height on precipitation and snow accumulation in idealized simulations, Journal of Geophysical Research: Atmospheres, 117, https://doi.org/10.1029/2011JD017052, 2012.

Held, I. M., Ting, M., and Wang, H.: Northern Winter Stationary Waves: Theory and Modeling, 2002.

Herrmann, A. D., Haupt, B. J., Patzkowsky, M. E., Seidov, D., and Slingerland, R. L.: Response of Late Ordovician paleoceanography to changes in sea level, continental drift, and atmospheric pCO_2: potential causes for long-term cooling and glaciation, Palaeogeography, Palaeoclimatology, Palaeoecology, 210, 385–401, https://doi.org/10.1016/j.palaeo.2004.02.034, 2004.

Holmden, C., Mitchell, C. E., LaPorte, D. F., Patterson, W. P., Melchin, M. J., and Finney, S. C.: Nd isotope records of late Ordovician sea-level change—Implications for glaciation frequency and global stratigraphic correlation, Palaeogeography, Palaeoclimatology, Palaeoecology, 386, 131–144, https://doi.org/10.1016/j.palaeo.2013.05.014, 2013.

Horton, D. E., Poulsen, C. J., and Pollard, D.: Orbital and CO_2 forcing of late Paleozoic continental ice sheets, Geophysical Research Letters, 34, https://doi.org/10.1029/2007GL031188, 2007.

Horton, D. E., Poulsen, C. J., and Pollard, D.: Influence of high-latitude vegetation feedbacks on late Palaeozoic glacial cycles, Nature Geosci, 3, 572–577, https://doi.org/10.1038/ngeo922, 2010.

https://doi.org/10.5194/egusphere-2026-1385
Preprint. Discussion started: 19 March 2026

Hurrell, J. W., Holland, M. M., Gent, P. R., Ghan, S., Kay, J. E., Kushner, P. J., Lamarque, J.-F., Large, W. G., Lawrence, D., Lindsay, K., Lipscomb, W. H., Long, M. C., Mahowald, N., Marsh, D. R., Neale, R. B., Rasch, P., Vavrus, S., Vertenstein, M., Bader, D., Collins, W. D., Hack, J. J., Kiehl, J., and Marshall, S.: The Community Earth System Model: A Framework for Collaborative Research, Bulletin of the American Meteorological Society, 94, 1339–1360, https://doi.org/10.1175/BAMS-D-12-00121.1, 2013.

Klockmann, M., Mikolajewicz, U., Kleppin, H., and Marotzke, J.: Coupling of the Subpolar Gyre and the Overturning Circulation During Abrupt Glacial Climate Transitions, Geophysical Research Letters, 47, e2020GL090361, https://doi.org/10.1029/2020GL090361, 2020.

Larour, E., Morlighem, M., Seroussi, H., Schiermeier, J., and Rignot, E.: Ice flow sensitivity to geothermal heat flux of Pine Island Glacier, Antarctica, Journal of Geophysical Research: Earth Surface, 117, https://doi.org/10.1029/2012JF002371, 2012.

Lee, H.-I., Mitchell, J. L., Lora, J. M., and Tripati, A.: Influence of Stationary Waves on Precipitation Change in North American Summer during the Last Glacial Maximum, https://doi.org/10.1175/JCLI-D-21-0886.1, 2023.

Li, X., Hu, Y., Guo, J., Lan, J., Lin, Q., Bao, X., Yuan, S., Wei, M., Li, Z., Man, K., Yin, Z., Han, J., Zhang, J., Zhu, C., Zhao, Z., Liu, Y., Yang, J., and Nie, J.: A high-resolution climate simulation dataset for the past 540 million years, Scientific Data, 9, 371, https://doi.org/10.1038/s41597-022-01490-4, 2022.

Liakka, J. and Lofverstrom, M.: Arctic warming induced by the Laurentide Ice Sheet topography, Climate of the Past, 14, 887–900, https://doi.org/10.5194/cp-14-887-2018, 2018.

Liakka, J., Löfverström, M., and Colleoni, F.: The impact of the North American glacial topography on the evolution of the Eurasian ice sheet over the last glacial cycle, Climate of the Past, 12, 1225–1241, https://doi.org/10.5194/cp-12-1225-2016, 2016.

Liu, P., Liu, Y., Peng, Y., Lamarque, J.-F., Wang, M., and Hu, Y.: Large influence of dust on the Precambrian climate, Nat Commun, 11, 4427, https://doi.org/10.1038/s41467-020-18258-2, 2020.

Löfverström, M. and Liakka, J.: On the limited ice intrusion in Alaska at the LGM, Geophysical Research Letters, 43, 11,030-11,038, https://doi.org/10.1002/2016GL071012, 2016.

Lowry, D. P., Poulsen, C. J., Horton, D. E., Torsvik, T. H., and Pollard, D.: Thresholds for Paleozoic ice sheet initiation, Geology, 42, 627–630, https://doi.org/10.1130/G35615.1, 2014.

Man, K., Wei, Q., Tan, N., Zhang, Z., Li, X., and Liu, Y.: Modeling the Cenozoic evolution of the Antarctic Ice Sheet-Influence of the uncertainty in climate forcing, Quaternary Sciences, 43, 911–924, https://doi.org/10.11928/j.issn.1001-7410.2023.04.01, 2023.

Melchin, M. J., Mitchell, C. E., Holmden, C., and Štorch, P.: Environmental changes in the Late Ordovician–early Silurian: Review and new insights from black shales and nitrogen isotopes, GSA Bulletin, 125, 1635–1670, https://doi.org/10.1130/B30812.1, 2013.

Montañez, I. P. and Poulsen, C. J.: The Late Paleozoic Ice Age: An Evolving Paradigm, Annu. Rev. Earth Planet. Sci., 41, 629–656, https://doi.org/10.1146/annurev.earth.031208.100118, 2013.

Oerlemans, J.: Some basic experiments with a vertically-integrated ice sheet model, Tellus, 33, 1–11, https://doi.org/10.1111/j.2153-3490.1981.tb01726.x, 1981.

Parish, T. R. and Cassano, J. J.: Diagnosis of the Katabatic Wind Influence on the Wintertime Antarctic Surface Wind Field from Numerical Simulations, Monthly Weather Review, 131, 1128–1139, https://doi.org/10.1175/1520-0493(2003)131<1128:DOTKWI>2.0.CO;2, 2003.

Pausata, F. S. R., Li, C., Wettstein, J. J., Kageyama, M., and Nisancioglu, K. H.: The key role of topography in altering North Atlantic atmospheric circulation during the last glacial period, Climate of the Past, 7, 1089–1101, https://doi.org/10.5194/cp-7-1089-2011, 2011.

Pohl, A., Donnadieu, Y., Le Hir, G., Ladant, J.-B., Dumas, C., Alvarez-Solas, J., and Vandenbroucke, T. R. A.: Glacial onset predated Late Ordovician climate cooling, Paleoceanography, 31, 800–821, https://doi.org/10.1002/2016PA002928, 2016.

Pohl, A., Lu, Z., Lu, W., Stockey, R. G., Elrick, M., Li, M., Desrochers, A., Shen, Y., He, R., Finnegan, S., and Ridgwell, A.: Vertical decoupling in Late Ordovician anoxia due to reorganization of ocean circulation, Nat. Geosci., 14, 868–873, https://doi.org/10.1038/s41561-021-00843-9, 2021.

Pollard, D.: A retrospective look at coupled ice sheet–climate modeling, Climatic Change, 100, 173–194, https://doi.org/10.1007/s10584-010-9830-9, 2010.

https://doi.org/10.5194/egusphere-2026-1385
Preprint. Discussion started: 19 March 2026

Pollard, D. and DeConto, R. M.: Description of a hybrid ice sheet-shelf model, and application to Antarctica, Geoscientific Model Development, 5, 1273–1295, https://doi.org/10.5194/gmd-5-1273-2012, 2012.
Reeh, N.: Parameterization of Melt Rate and Surface Temperature in the Greenland Ice Sheet, Polarforschung, 59, 113–128, https://doi.org/10.2312/polarforschung.59.3.113, 1991.
Saupe, E. E., Qiao, H., Donnadieu, Y., Farnsworth, A., Kennedy-Asser, A. T., Ladant, J.-B., Lunt, D. J., Pohl, A., Valdes, P., and Finnegan, S.: Extinction intensity during Ordovician and Cenozoic glaciations explained by cooling and palaeogeography, Nat. Geosci., 13, 65–70, https://doi.org/10.1038/s41561-019-0504-6, 2020.
Scherrenberg, M. D. W., Berends, C. J., Stap, L. B., and van de Wal, R. S. W.: Modelling feedbacks between the Northern Hemisphere ice sheets and climate during the last glacial cycle, Climate of the Past, 19, 399–418, https://doi.org/10.5194/cp-19-399-2023, 2023.
Scotese, C. R., Song, H., Mills, B. J. W., and van der Meer, D. G.: Phanerozoic paleotemperatures: The earth's changing climate during the last 540 million years, Earth-Science Reviews, 215, 103503, https://doi.org/10.1016/j.earscirev.2021.103503, 2021.
Sheehan, P. M.: History of marine biodiversity, Geological Journal, 36, 231–249, https://doi.org/10.1002/gj.890, 2001.
Thornton, P. E., Lamarque, J.-F., Rosenbloom, N. A., and Mahowald, N. M.: Influence of carbon-nitrogen cycle coupling on land model response to CO_2 fertilization and climate variability, Global Biogeochemical Cycles, 21, https://doi.org/10.1029/2006GB002868, 2007.
Torsvik, T. H. and Cocks, L. R. M.: Earth History and Palaeogeography, Cambridge University Press, Cambridge, https://doi.org/10.1017/9781316225523, 2016.
Trotter, J. A., Williams, I. S., Barnes, C. R., Lécuyer, C., and Nicoll, R. S.: Did Cooling Oceans Trigger Ordovician Biodiversification? Evidence from Conodont Thermometry, Science, 321, 550–554, https://doi.org/10.1126/science.1155814, 2008.
Vandenbroucke, T. R. A., Armstrong, H. A., Williams, M., Zalasiewicz, J. A., and Sabbe, K.: Ground-truthing Late Ordovician climate models using the paleobiogeography of graptolites, Paleoceanography, 24, https://doi.org/10.1029/2008PA001720, 2009.
Vihma, T., Tuovinen, E., and Savijärvi, H.: Interaction of katabatic winds and near-surface temperatures in the Antarctic, Journal of Geophysical Research: Atmospheres, 116, https://doi.org/10.1029/2010JD014917, 2011.
Vizcaíno, M., Mikolajewicz, U., Jungclaus, J., and Schurgers, G.: Climate modification by future ice sheet changes and consequences for ice sheet mass balance, Clim Dyn, 34, 301–324, https://doi.org/10.1007/s00382-009-0591-y, 2010.
Warthen, S. T.: Attempting to Recreate the Late Ordovician Glaciation with the University of Victoria Earth System Climate Model, The Ohio State University, 2016.
Wei, Q., Liu, Y., Yan, Q., Yao, T., Wang, M., Huang, H., and Hu, Y.: The Glacier-Climate Interaction Over the Tibetan Plateau and Its Surroundings During the Last Glacial Maximum, Geophysical Research Letters, 50, e2023GL103538, https://doi.org/10.1029/2023GL103538, 2023.
Zhu, J., Liu, Z., Zhang, X., Eisenman, I., and Liu, W.: Linear weakening of the AMOC in response to receding glacial ice sheets in CCSM3, Geophysical Research Letters, 41, 6252–6258, https://doi.org/10.1002/2014GL060891, 2014.